A New Leaky Waveguide for Millimeter Waves Using Nonradiative Dielectric (NRD) Waveguide—Part I: Accurate Theory

ALBERTO SANCHEZ, MEMBER, IEEE, AND ARTHUR A. OLINER, LIFE FELLOW, IEEE

Abstract —**An almost-rigorous analysis is presented for a new leaky waveguide of simple configuration based on a recent nonradiative modification of *H* guide suitable for millimeter wavelengths. The analysis employs a transverse equivalent network that yields a dispersion relation in closed form, and contains some interesting and subtle features. Numerical values are presented for the phase and leakage constants in terms of the different geometric parameters and the dielectric constant; comparisons with measurements are made in the companion paper, part II.**

I. Introduction

THIS INVESTIGATION was motivated by a search for new types of leaky-wave antennas for millimeter waves. At those shorter wavelengths, waveguide losses increase and structures become harder to fabricate in view of the reduced size. To overcome those difficulties, we selected a leaky-wave structure that is simple in form, uniform longitudinally, and based on a low-loss waveguide. Even though the application is to antennas, the method of analysis employs microwave network techniques of direct interest to microwave engineers. Furthermore, this antenna is essentially a modification of the waveguide itself and it can be integrated directly with the remainder of the circuitry.

Two papers appeared recently [1], [2] which proposed a new type of waveguide for millimeter waves, and showed that various components based on it can be readily designed and fabricated. The simple but basic modification introduced by the authors, Yoneyama and Nishida, transformed the old, well-known *H* guide into a potentially practical waveguide with attractive features. The old *H* guide stressed its potential for low-loss long runs of waveguide by making the space between the metal plates large, certainly greater than half a wavelength; as a result, the waveguide had lower loss, but any discontinuities or bends in it would produce leakage of power away from the guide. Yoneyama and Nishida observed simply that when the spacing is reduced to less than half a wavelength, all the bends and discontinuities become purely reactive; they therefore call their guide "nonradiative dielectric waveguide," or NRD guide. As a result of this modification, many components can be constructed easily and in an integrated circuit fashion, and these authors proceeded to demonstrate how to fabricate some of them, such as feeds, terminations, ring resonators, and filters [2], [3].

These papers [1], [2] treat only reactive circuit components, and no mention is made of how this type of waveguide can be used in conjunction with *antennas*. The present paper serves two functions. First, it shows that a leaky-wave antenna can be readily fabricated with "nonradiative dielectric waveguide," and, in fact, that it can be directly connected to the above-mentioned circuits in integrated circuit fashion if desired. Second, it presents a very accurate theory for the leakage and phase constants of the antenna. A key feature of this theory involves an almost-rigorous transverse equivalent network, which requires two coupled transmission lines. Some subtle features are involved in the derivation of the elements of this equivalent network, including the best choice of constituent transverse modes, an analytic continuation into the below-cutoff domain, and mode coupling at an air–dielectric interface. In the discussion below, we present the structure of the antenna, the principle of operation, the almost-rigorous theory, and typical numerical examples that can serve as guides for antenna performance.

The form of the antenna is also responsive to problems facing line-source antennas at millimeter wavelengths; that is, the antenna is simple to fabricate since it is composed of a single continuous open slit. It is fed by a relatively low-loss waveguide so that the leakage constant of the antenna dominates over the attenuation constant of the waveguide due to material losses. The antenna is also simple to design because it is possible to vary the leakage constant without measurably affecting the phase constant and because our theory yields *closed-form expressions* for the leakage and phase constants.

A somewhat similar antenna was analyzed and measured some time ago by Shigesawa and Takiyama [5]–[8], but it was based on *H* guide rather than NRD guide. Nevertheless, the mechanism for leakage is basically the

Manuscript received November 25, 1986; revised April 3, 1987. This work was supported in part by the Rome Air Development Center at Hanscom AFB, MA, under Contract F19628-81-K-0044.

A. Sanchez is with RCA Astro-Space Division, Princeton, NJ 08543-0800.

A. A. Oliner is with the Polytechnic University, Brooklyn, NY 11201.

IEEE Log Number 8715411.

same as ours, employing a foreshortening of outer walls; this antenna concept, although conceived independently by us recently, should therefore be credited to them. Their use of H guide rather than NRD guide made their antenna less practical, however, since substantial radiation occurred from their feed arrangement itself. In addition, their antenna radiated from both sides, whereas ours radiates from only one side. The leakage from their feeding arrangement also produced substantial errors in their measured data, since they employed an indirect (insertion loss) method for determining the leakage constant. Their theory was also approximate whereas ours is almost rigorous, and their theory did not agree very well with their measurements. In sum, they conceived of the antenna type first, but our actual structure is more practical, and our theory and our measurements are both accurate and agree very well with each other.

The present paper, part I, discusses the new leaky waveguide and its principle of operation, derives an accurate theory for its characteristics, and presents numerical values for its behavior. The companion paper, part II, presents the *measurement* phase of this investigation. In that paper, we describe the experimental approach and the measurement setup, and we then present detailed comparisons between accurate theoretical calculations and these measured results. It is shown that *very good agreement* is obtained between the measured and theoretical values over a large range of working parameters.

II. Principle of Operation of the Leaky Waveguide

The new waveguide, shown in Fig. 1, looks like the earlier H guide except that the spacing between the plates is less than half a wavelength to ensure the nonradiative feature. In the vertical (y) direction, the field is of the standing wave form in the dielectric region and is exponentially decaying in the air regions above and below. The guided wave propagates in the axial (z) direction. The leaky-wave antenna based on this waveguide is shown in Fig. 2 (a), where we see that the antenna is created simply by decreasing the distance d between the dielectric strip and the top of the metal plates. When distance d is small, the fields have not decayed to negligible values at the upper open end, and, therefore, some power leaks away. The upper open end forms the antenna aperture, and the aperture distribution is tapered by varying the distance d as a function of the longitudinal variable z. The polarization of the antenna is seen to be vertical in view of the principal electrical field orientation in the waveguide. Because of the hybrid nature of the basic mode, however, there is also some cross-polarized (horizontally polarized) radiation in (split) off-axis beams, but not in the principal plane (the yz plane).

The antenna is seen to be very simple in structure. A side view of the antenna, shown in Fig. 2(b), indicates that the taper in the antenna amplitude distribution (required for sidelobe control) is achieved easily by positioning the dielectric strip waveguide with respect to the upper open end, and also that the feeding strip can be readily connected to some other part of the millimeter-wave circuit and, therefore, can serve as the output from it.

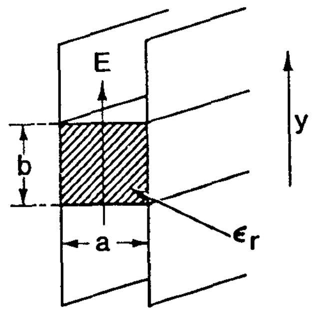

Fig. 1. Cross section view of nonradiative dielectric waveguide, where $a < \lambda_0/2$.

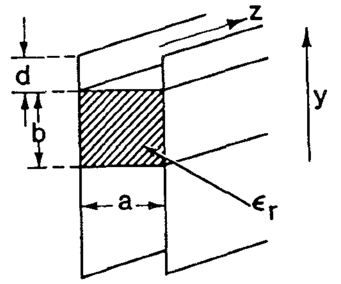

(a)

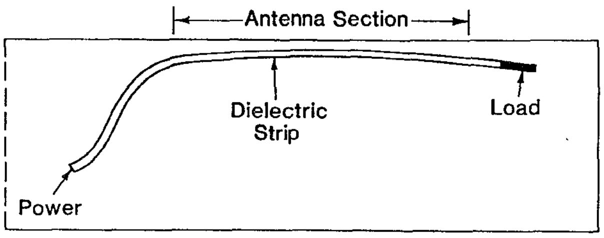

(b)

Fig. 2 (a) Cross section view of leaky-wave structure where leakage is controlled by distance d. (b) Side view of the leaky waveguide with tapering.

III. Almost-Rigorous Transverse Equivalent Network

A. Summary

The antenna is analyzed as a leaky waveguide that possesses a complex propagation constant $\beta - j\alpha$, where β is the phase constant and α is the attenuation constant or leakage constant. It can be shown that the knowledge of β and α as a function of the geometric parameters is sufficient to permit the complete design of the leaky-wave antenna in accordance with the prescribed radiation requirements. We thus establish a transverse equivalent network for the cross section of the antenna, and from the resonance of this network we obtain the dispersion relation for the β and α values. An almost-rigorous equivalent network is presented in Fig. 3, where it is seen that two coupled transmission lines are required in the representation. The reason for the two lines is that the waveguide modes are hybrid and possess all six field components in the presence of the radiating open end.

If we employ the usual TE and TM modes in these transmission lines, which represent the constituent transverse modes, the lines will remain uncoupled at the air–dielectric interface but will be coupled together at the radiating open end. On the other hand, the open end is uniform longitudinally, and this geometrical arrangement suggests the use of $E^{(z)}$-type and $H^{(z)}$-type modes (alternatively called LSM and LSE modes, respectively, with respect to the xy plane). Transmission lines representing such modes will not couple at the radiating open end, but do become coupled at the air–dielectric interface. These two valid but alternative representations were considered, and we chose the second of these as the simpler approach for our antenna.

The transverse equivalent network in Fig. 3 is thus based on the $E^{(z)}$-type and $H^{(z)}$-type transverse modes mentioned above. The coupling network at the air–dielectric interface was obtained from an adaptation of a network presented earlier [4] for cylindrical air–dielectric interfaces, and suitably transformed for planar interfaces. Its derivation and utilization in planar form are new.

The principal new feature in the transverse equivalent network in Fig. 3 relates to the terminal admittance and impedance representing the $E^{(z)}$-type and $H^{(z)}$-type modes incident on the radiating open end. Those immittances were not available in the literature but were derived by analytic continuation of expressions for reflection coefficients given by Weinstein [9]. Those reflection coefficients applied to normal incidence of ordinary parallel-plate modes; modifications were made to account for modes below cutoff and then for a longitudinal wavenumber variation (corresponding to oblique incidence), the former step producing results which appear totally different since the phases and amplitudes of the reflection coefficients then become exchanged.

The terminal immittances in Fig. 3 assume that all higher modes in the transmission lines decay exponentially to infinity. In principle, they "see" the air–dielectric interface a distance d away. In practice, that distance is electrically large; for example, for the first higher mode in a specific case the field at the air–dielectric interface was about 30 dB lower than its value at the radiating open end. Because of this feature, however, we refer to this analysis as *almost-rigorous*, rather than rigorous.

B. The Modes Employed

The coordinate system to be used appears in connection with Fig. 4. The final leaky wave propagates in the axial (z) direction, and the transverse transmission line direction is the vertical (y) direction. The transmission direction of the transverse modes is thus the y direction. However, the structure is uniform with respect to the z direction. The E-type and H-type modes to be employed in the transverse representation are, therefore, separable with respect to z, but propagating in y. It is accurate, therefore, to designate them as $E^{(z)}$-type and $H^{(z)}$-type

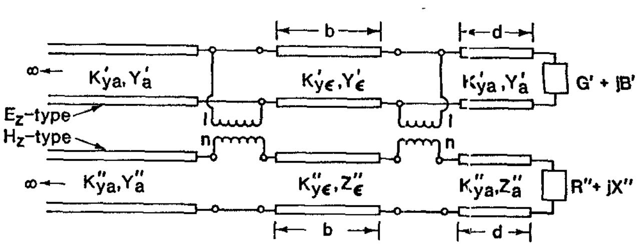

Fig. 3. Rigorous transverse equivalent network for the structure shown in Fig. 2(a). The network is placed on its side for clarity.

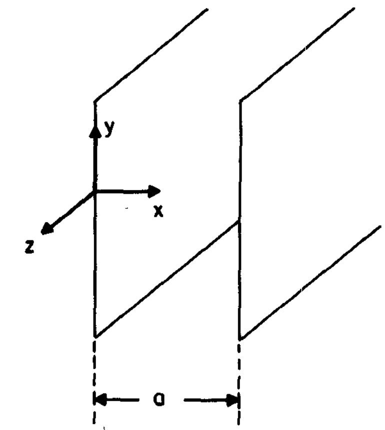

Fig. 4. Parallel-plate waveguide and associated coordinate system.

modes (or, alternatively, as LSM and LSE modes with respect to the xy plane).

We shall choose the E-type and H-type notation, and follow the formulation developed by Altschuler and Goldstone [12] but with our coordinate system. They presented the derivations of the pertinent field relations and the orthogonality relations, so we will not repeat them here. However, it is necessary for us to know the field components and the characteristic impedances for these modes corresponding to our choice of coordinate system. The constituent vertical guiding regions in our antenna structure, shown in Fig. 2(a), are portions of *parallel-plate waveguide*, either dielectric-filled or air-filled. We also recall that ordinary TM (or E) and TE (or H) modes propagating in the y direction would be characterized by the presence or absence of the y component of field, whereas these E-type and H-type modes are distinguished by the presence or absence of the appropriate z component.

The E-type modes shall be denoted by primed quantities and the H-type modes by double-primed quantities. The transmission direction is y, so that the components of the mode functions for the ith E-type modes are h'_{xi}, e'_{xi}, and e'_{zi}, with $h'_{zi}=0$. Correspondingly, the components of the mode functions for the ith H-type modes are e''_{xi}, h''_{xi}, and h''_{zi}, with $e''_{zi}=0$. For the air-filled regions, the relations between them and the expressions for the characteristic immittances Z'_i and Y''_i are

$E^{(z)}$-type modes:

$$h'_{zi}=0 \qquad h'_{xi}=e'_{zi} \qquad e'_{xi}=\frac{1}{k_0^2-k_{zi}^2}\frac{\partial^2 e'_{zi}}{\partial x\,\partial z} \tag{1}$$

$$Z'_i=\frac{k_0^2-k_{zi}^2}{\omega\epsilon_0 k'_{yi}} \tag{2}$$

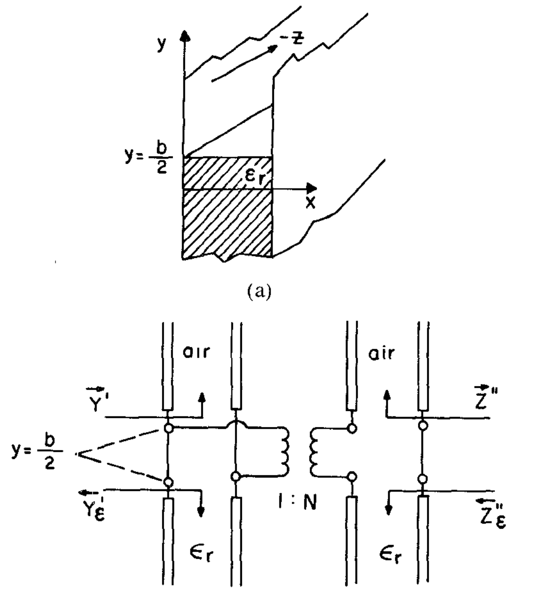

Fig 5. (a) Infinite parallel-plate waveguide showing one air–dielectric intervace. (b) Transverse equivalent network for the air–dielectric interface in the inhomogeneously filled parallel-plate waveguide shown in (a).

$H^{(z)}$-type modes:

$$e''_{zi}=0 \qquad e''_{xi}=h''_{zi} \qquad h''_{xi}=\frac{1}{k_0^2-k_{zi}^2}\frac{\partial^2 h''_{zi}}{\partial x\,\partial z} \tag{3}$$

$$Y_i''=\frac{k_0^2-k_{zi}^2}{\omega\mu_0 k''_{yi}}. \tag{4}$$

The explicit field components for the *parallel-plate* waveguide constituent regions, under the condition that a net traveling wave propagates along the z direction, so that $\partial/\partial z$ yields $-j\beta$, where $k_z=\beta$, are given in the Appendix.

C. The Air–Dielectric Interface

We note from the structure depicted in Fig. 2(a) that two air–dielectric interfaces appear in the cross section when viewed in the y direction. One of these interfaces is shown in Fig. 5(a).

If the ordinary TE and TM modes were employed in the y direction, the air–dielectric interface would represent a simple junction between transmission lines, and the TE and TM modes would not be coupled together at the interface. For the E-type and H-type modes we employ, however, these modes do couple at the interface, and the purpose of this section is to derive a simple network to describe this coupling.

A coupling network of this type was derived previously by Clarricoats and Oliner [4] for the inhomogeneously filled circular waveguides. There, the geometry was radial, and the transmission lines were the so-called E-type and H-type radial transmission lines developed by Marcuvitz [10]. These radial transmission lines represent propagation in the radial direction, but are found to be separable with respect to the axial direction. In our case, the geometry is planar rather than cylindrical; the modes propagate in y but are separable with respect to the z (axial) direction. The strong similarities present suggest that the procedure introduced there can be adapted for use here, and indeed this turns out to be the case.

The boundary conditions that must be satisfied at the air–dielectric interface are

$$\begin{aligned} \boldsymbol{E}_{t\epsilon}&=\boldsymbol{E}_t\\ \boldsymbol{H}_{t\epsilon}&=\boldsymbol{H}_t \end{aligned} \tag{5}$$

that is, the tangential electric and magnetic fields must be continuous across the interface. In terms of components, relations (5) become

$$\begin{aligned} \boldsymbol{x}_0(E'_{x\epsilon}+E''_{x\epsilon})+z_0E'_{z\epsilon}&=\boldsymbol{x}_0(E'_x+E''_x)+z_0E'_z\\ \boldsymbol{x}_0(H'_{x\epsilon}+H''_{x\epsilon})+z_0H''_{z\epsilon}&=\boldsymbol{x}_0(H'_x+H''_x)+z_0H''_z \end{aligned} \tag{6}$$

where $\boldsymbol{x}_0$ and z_0 are unit vectors and the arguments of the components are dropped for simplicity. Expressing (6) in terms of mode functions, and equating the $\boldsymbol{x}_0$ components and the z_0 components separately, we obtain

$$\begin{aligned} V''_\epsilon e''_{x\epsilon}+V'_\epsilon e'_{x\epsilon}&=V''e''_x+V'e'_x\\ V'_\epsilon e'_{z\epsilon}&=V'e'_z \end{aligned} \tag{7}$$

$$\begin{aligned} I''_\epsilon h''_{x\epsilon}+I'_\epsilon h'_{x\epsilon}&=I''h''_x+I'h'_x\\ I''_\epsilon h''_{z\epsilon}&=I''h''_z. \end{aligned} \tag{8}$$

Upon examination of the mode functions (A1) to (A3) and (A7) to (A9) of the Appendix, we find that

$$\begin{aligned} e'_{z\epsilon}&=e'_z \qquad & h''_{z\epsilon}&=h''_z\\ h'_{x\epsilon}&=h'_x \qquad & e''_{x\epsilon}&=e''_x\\ e'_{x\epsilon}&\neq e'_x \qquad & h''_{x\epsilon}&\neq h''_x. \end{aligned} \tag{9}$$

On use of (9), relations (7) and (8) reduce to

$$\begin{aligned} V'_\epsilon&=V'\\ I''_\epsilon&=I'' \end{aligned} \tag{10}$$

$$\begin{aligned} V''_\epsilon-V''&=V'\frac{e'_x-e'_{x\epsilon}}{e''_x}\\ I'_\epsilon-I'&=I''\frac{h''_x-h''_{x\epsilon}}{h'_x}. \end{aligned} \tag{11}$$

When the relations in (11) are divided by I'' and V', respectively, and use is made of (10), (11) becomes

$$\begin{aligned} \frac{V''_\epsilon}{I''_\epsilon}-\frac{V''}{I''}&=\frac{V'}{I''}\frac{e'_x-e'_{x\epsilon}}{e''_x}\\ \frac{I'_\epsilon}{V'_\epsilon}-\frac{I'}{V'}&=\frac{I''}{V'}\frac{h''_x-h''_{x\epsilon}}{h'_x}. \end{aligned} \tag{12}$$

The two equations (12) can be multiplied together, eliminating the ratio V'/I'' and yielding

$$\left(\frac{V''_\epsilon}{I''_\epsilon}-\frac{V''}{I''}\right)\left(\frac{I'_\epsilon}{V'_\epsilon}-\frac{I'}{V'}\right)=\frac{h''_x-h''_{x\epsilon}}{h'_x}\frac{e'_x-e'_{x\epsilon}}{e''_x}. \tag{13}$$

Finally, (13) can be rewritten as

$$\left(\overleftarrow{Z}''_\epsilon+\overrightarrow{Z}''\right)\left(\overleftarrow{Y}'_\epsilon+\overrightarrow{Y}'\right)=N^2 \tag{14}$$

where $\overleftarrow{Z}_\epsilon''$ and $\overleftarrow{Y}_\epsilon'$ are the impedance of the H-type mode and the admittance of E-type mode at the air–dielectric interface looking into the dielectric region, and $\overrightarrow{Z}''$ and $\overrightarrow{Y}'$ are the corresponding quantities looking into the air region. We recall that a change in sign results when an impedance or admittance is taken looking in the opposite direction.

A simple network form, shown in Fig. 5(b), can be drawn based on (14) which is representative of the coupling between the E-type and H-type modes at the air–dielectric interface. The turns ratio N in this network is then given by

$$N^2 = \frac{h_x'' - h_{x\epsilon}''}{h_x'} \frac{e_x' - e_{x\epsilon}'}{e_x''}. \tag{15}$$

When expressions (A1), (A3), (A8), and (A9) are used for the mode functions in (15), we obtain for the turns ratio N

$$N = \frac{k_0^2(\epsilon_r - 1)\beta(\pi/a)}{(k_0^2 - \beta^2)(\epsilon_r k_0^2 - \beta^2)}. \tag{16}$$

The network in Fig. 5(b) can be used as a constituent in a transverse equivalent network that is representative of the H guide or NRD guide structure shown in Fig. 1. A transverse resonance equation can then be set up using E-type and H-type modes, utilizing relations (16) for N and (A4) and (A10) of the Appendix for the appropriate characteristic immittances of the transmission lines. Sanchez [11] has shown that the dispersion relation derived in this fashion reduces readily to the one given in the literature and found by employing the usual TM mode in the y direction. It is a cumbersome method for that simple problem, but it is indeed mathematically equivalent to the standard procedure.

D. The Radiating Open End

If ordinary TE and TM modes with axial (z) variation are incident on the open end of parallel-plate guide, they become coupled by the discontinuity. The modes remain uncoupled, though, when $E^{(z)}$-type and $H^{(z)}$-type modes are employed instead. In obtaining the terminal complex immittances for these modes, which are needed in the transverse equivalent network, we are able to make use of the expressions for reflection coefficients derived by Weinstein [9] for a simpler situation.

His results apply to *propagating* TM_1 (or E_1) and TE_1 (or H_1) modes in parallel-plate guide *normally* incident on the radiating open end. Our case involves modes with longitudinal variation along z which are below cutoff, so that it was necessary to *analytically continue* Weinstein's results in an appropriate manner. His expressions are of great value, however, since they were derived using the factorization, or Wiener–Hopf, method, and are therefore rigorous.

The analytical continuation required two steps. First, we recall that for NRD guide it is necessary to maintain plate spacing of less than half a wavelength so that the incident modes will be below cutoff even in the absence of axial variation. This circumstance calls for an analytic continuation of Weinstein's reflection coefficients to modes below cutoff.

The next step accounts for the longitudinal variation of the incident $E^{(z)}$-type and $H^{(z)}$-type modes. These modes become the normally incident TE_1 and TM_1 modes, respectively, when $\beta = 0$ in expressions (A1) to (A12) of the Appendix. The paper by Altschuler and Goldstone [12] has also indicated how reflection coefficients must be modified when a longitudinal variation is introduced into the E-type and H-type modes, provided that these modes remain uncoupled by the discontinuity in question, as is the case here. The modification is to replace k_0 wherever it appears by $(k_0^2 - \beta^2)^{1/2}$.

1) Summary of Weinstein's Formulation: Weinstein's rigorous analysis [9] applies to TM and TE modes normally incident on the open end of parallel-plate guide. He solves for the reflection coefficients of the surface currents in each case, but we can relate these to the modal voltage and current reflection coefficients of interest in our problem. His coordinate system, time dependence, and other notation are also different.

In his notation, the reflection coefficients are written as

$$R_{1,1} = -|R_{1,1}|e^{-j\theta} \tag{17}$$

where

$$|R_{1,1}|_{H_1} = \sqrt{(q-\gamma)/(q+\gamma)}\, e^{-\pi\gamma} = |R_{1,1}''| \tag{18}$$

$$|R_{1,1}|_{E_1} = \sqrt{(q+\gamma)/(q-\gamma)}\, e^{-\pi\gamma} = |R_{1,1}'| \tag{19}$$

and

$$q = a/\lambda \qquad \gamma = k_y(a/2\pi) = \sqrt{q^2 - 1/4}. \tag{20}$$

Quantity θ is also given for both mode types by

$$\theta = 2\Bigg[2 - C + \ln(2/q) - (1/2\gamma)\sin^{-1}(\gamma/q) - (1/\gamma)\sin^{-1}(\gamma/\sqrt{2}) + \sigma - \sum_{m=1}^{m=\infty} A_{2m+1}S_m\gamma^{2m}\Bigg] \tag{21}$$

where

$$C = 0.577\cdots = \lim_{N\to\infty}\left(\sum_{n=1}^{n=N} 1/n - \ln N\right)$$

$$\sigma = 0.265\cdots = \sum_{n=3}^{n=\infty}\left[1/(n-1) - 1/\sqrt{n(n-1)}\right] \tag{22}$$

and A_{2m+1} are the coefficients of the series

$$\sin^{-1} x = \sum_{m=0}^{m=\infty} A_{2m+1}x^{2m+1} \tag{23}$$

where $A_1 = 1$, $A_3 = 1/6$, $A_5 = 3/40\cdots$ and S_m is given by

$$S_m = \sum_{n=3}^{n=\infty} 1/[n(n-1)]^{m+1/2} \tag{24}$$

with $S_1 = 0.123$, $S_2 = 0.014, \cdots$.

We find above what is customary in these factorization procedures, that the magnitudes are simple in form but the phase expressions are complicated.

We next need to relate these reflection coefficients for the wall current densities to the modal voltage and current reflection coefficients corresponding to our transmission line formulation. In this connection, we may write [13] for the TE_1 (or H_1) mode

$$j_z = H_y|_{\text{wall}} = (1/j\omega\mu)\nabla_t \cdot (y_0 \times E_t) \tag{25}$$

where the time dependence is $\exp(j\omega t)$. Since

$$E_t = V(y)e_t(x)$$

we see that the reflection coefficient for the current density j_z is also the voltage reflection coefficient. Consequently,

$$R_V'' = -|R_{1,1}''|e^{-j\theta} \tag{26}$$

for the TE_1 (or H_1) mode, where $|R_{1,1}''$ and θ are still given by (18) and (21), and the double prime is employed because of the mode involved.

For the TM_1 (or E_1) mode, we may write [13]

$$j_y = -H_z|_{\text{wall}} = -I(y)h_z(x). \tag{27}$$

Therefore, the reflection coefficient for the current density for this mode corresponds to the current reflection coefficient

$$R_I' = -|R_{1,1}'|e^{-j\theta} \tag{28}$$

where $|R_{1,1}'|$ and θ are still given by (19) and (21).

It was indicated in (20) how q and γ are related to frequency and wavenumbers in our notation. Elaborating further, we find

$$q = a/\lambda_0 = (k_0 a)/(2\pi) \qquad \gamma = (k_y a)/(2\pi) \tag{29}$$

so that $\gamma = \sqrt{q^2 - 1/4}$ becomes

$$k_y = \sqrt{k_0^2 - (\pi/a)^2} \tag{30}$$

and factors found in (18) and (19) become

$$\sqrt{(q \mp \gamma)/(q \pm \gamma)} = \sqrt{(k_0 \mp k_y)/(k_0 \pm k_y)} \equiv \begin{matrix} r_{1,1}'' \\ r_{1,1}' \end{matrix} \tag{31}$$

which we have called $r_{1,1}''$ and $r_{1,1}'$ for simplicity in the following discussion.

2) Analytic Continuations: The first step is to analytically continue the expressions for the reflection coefficients so that they apply to *modes below cutoff*. The term γ in (29) is now imaginary and should be written as $\gamma = -j|\gamma|$. The expression for the phase angle is not ambiguous if principal values are taken for the terms $\ln(2/q)$, $\sin^{-1}(\gamma/q)$, and $\sin^{-1}(\gamma/\sqrt{2})$. We need only to be careful in the choice of branches in the complex plane for the factors $r_{1,1}''$ and $r_{1,1}'$ since $e^{+j\pi|\gamma|}$ is not ambiguous either.

In Fig. 6(a) and (b), we draw the three mappings that are involved in ascertaining the choice of branches that correctly analytically continue the reflection coefficient magnitudes $|R_{1,1}'|$ and $|R_{1,1}''|$.

a) The mapping $q \to \gamma$ maps the segments of real axis $1/2 < q < 3/2$ and $0 < q < 1/2$ onto the segments $0 < \gamma < \sqrt{2}$ of the real axis of the γ plane and the segment of the imaginary γ axis between 0 and $(-1/2)j$, respectively. We recognize that $q = 1/2$ corresponds to mode cutoff.

b) The mapping $q \to r_{1,1}'$ maps the segment of the real axis $1/2 < q < 3/2$ onto the segment of the real axis of the $r_{1,1}'$ plane between 1 and $C' = [(3+2\sqrt{2})/(3-2\sqrt{2})]^{1/2} > 1$, and the real segment $0 < q < 1/2$ onto the arcs of unit circle subtended by the second and fourth quadrants.

c) In a similar manner, the mapping $q \to r_{1,1}''$ maps the segment of the real axis $1/2 < q < 3/2$ onto the segment of the real axis of the plane $r_{1,1}''$ between 1 and $C'' = [(3-$

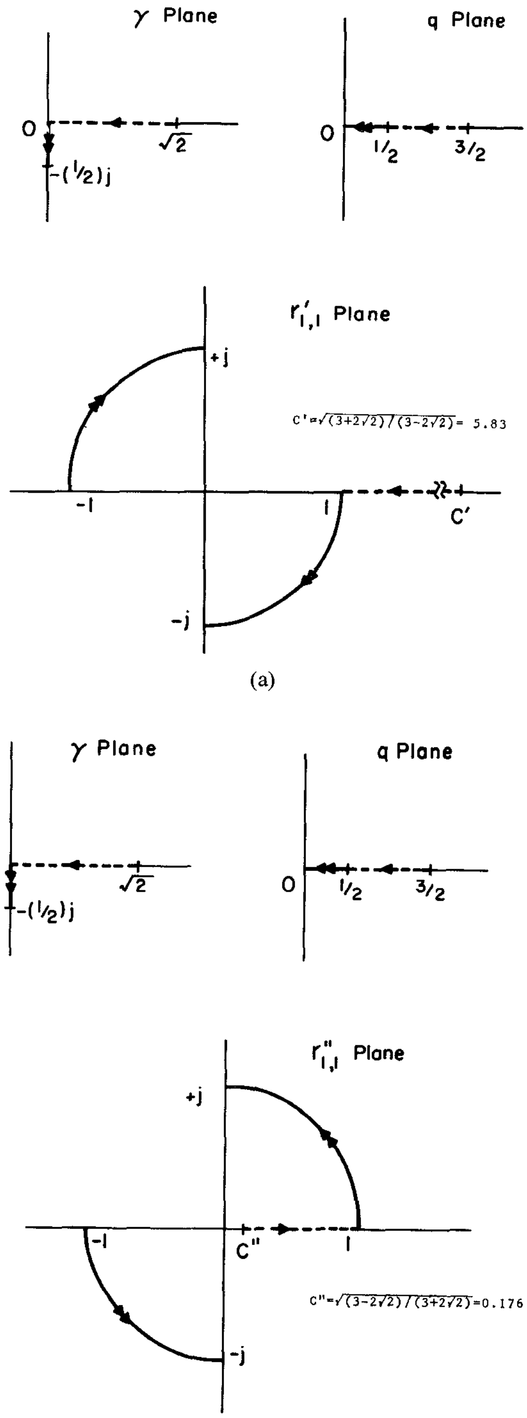

Fig. 6. (a) The $q \to \gamma$ and $q \to r_{1,1}'$ mappings. (The single and double arrows refer to different segments associated with the mappings.) (b) The $q \to \gamma$ and $q \to r_{1,1}''$ mappings.

$2\sqrt{2})/(3+2\sqrt{2})]^{1/2}<1$, and the real segment $0<q<1/2$ onto the arcs of unit circle subtended by the first and third quadrants.

The continuity condition of the mappings $|R'_{1,1}|$ and $|R''_{1,1}|$ at $q=1/2$ along the real axis of the q plane imposes the choices of the arcs of unit circle situated in the fourth and first quadrants as the correct analytical continuation of the $r'_{1,1}$ and $r''_{1,1}$ quantities. Thus,

$$\mathrm{Re}\left(\sqrt{(q\pm\gamma)/(q\mp\gamma)}\right)>0$$

when the mode just goes below cutoff.

Until now, we have not taken into account the *variation with z* that is present in our problem. When we include this variation, the TM_1 and TE_1 modes treated above become the $H^{(z)}$-type and $E^{(z)}$-type modes of concern to us. To determine the effect of this variation with z, we change q to q', where

$$q=k_0(a/2\pi) \qquad q'=\left(k_0^2-\beta^2\right)^{1/2}(a/2\pi). \quad (32)$$

From (26), bearing in mind that the voltage reflection coefficient is the negative of the current reflection coefficient, we have

$$-\Gamma'_I=\Gamma'_V=\left(R''_{1,1}\right)_V\Big|_{q'}=-|R''_{1,1}e^{-j\theta}|_{q'} \quad (33)$$

while from (28)

$$-\Gamma''_V=\Gamma''_I=\left(R'_{1,1}\right)_I\Big|_{q'}=-|R'_{1,1}|e^{-j\theta}\Big|_{q'}. \quad (34)$$

The terminal impedance for the $H^{(z)}$-type mode and the terminal admittance for the $E^{(z)}$-type mode corresponding to the radiating open end are, therefore, given by

$$Z''_L=\frac{k_y}{\omega\epsilon_0}\frac{1+\Gamma''_V}{1-\Gamma''_V}=\frac{\sqrt{k_0^2-(\pi/a)^2-\beta^2}}{\omega\epsilon_0}\frac{1+\Gamma''_V}{1-\Gamma''_V} \quad (35)$$

$$Y'_L=\frac{k_y}{\omega\mu_0}\frac{1+\Gamma'_I}{1-\Gamma'_I}=\frac{\sqrt{k_0^2-(\pi/a)^2-\beta^2}}{\omega\mu_0}\frac{1+\Gamma'_I}{1-\Gamma'_I}. \quad (36)$$

It should be remarked that the characteristic impedance $k_y/\omega\epsilon_0$ and admittance $k_y/\omega\mu_0$ appearing in the last two equations are the ones for the E_1 and H_1 modes when k_0^2 is replaced by $k_0^2-\beta^2$ and not the ones corresponding to the $H^{(z)}$-type and $E^{(z)}$-type modes. In the transverse equivalent network given in Fig. 3, Z''_L and Y'_L are written, respectively, as $R''+jX''$ and $G'+jB'$.

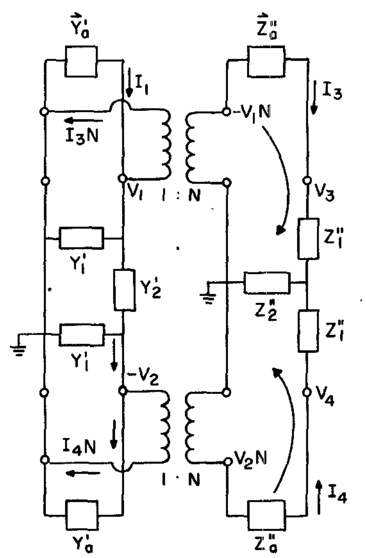

Fig. 7. Complete network showing the sign conventions used in (37). Transmission lines are replaced by their equivalent lumped elements.

E. Complete Transverse Equivalent Network

Once the equivalent networks for the air–dielectric interface and the open-ended parallel-plate guide are found, the transverse equivalent network of the leaky-wave antenna shown in Fig. 2(a) can be established as shown in Fig. 3.

The equivalent network in Fig. 3 is redrawn in Fig. 7 with lumped element equivalences of the transmission lines corresponding to the dielectric strip. The transmission lines of length d are included in immittances $\vec{Y}'_a$ and $\vec{Z}''_a$, which are defined in (39) and (40).

This network is analyzed via a hybrid method, where nodal equations are written for nodes 1 and 2 whereas mesh equations are used for meshes 3 and 4:

$$\begin{aligned}
&(\vec{Y}'_a+Y'_1+Y'_2)V_1 + Y'_2V_2 + NI_3 = 0\\
&Y'_2V_1+(Y'_a+Y'_1+Y'_2)V_2 - NI_4=0\\
&NV_1 + (\vec{Z}''_a+Z''_1+Z''_2)I_3 + Z''_2I_4=0\\
&-NV_2 + Z''_2I_3+(Z''_a+Z''_1+Z''_2)I_4=0.
\end{aligned} \quad (37)$$

The ambiguity in sign of the transformer terminal magnitudes was resolved by taking the sign convention that was used in [4]; this choice in (37), when applied to the simpler H guide case, for which $d=\infty$, led to an equation of the form (14).

F. The Dispersion Relation for the Leaky Mode

The dispersion relation is found with the help of the usual method, i.e., by writing the compatibility condition for the homogeneous system of equations (37). By doing so, one obtains

$$\begin{vmatrix}
\vec{Y}'_a+Y'_1+Y'_2 & Y'_2 & N & 0\\
Y'_2 & Y'_a+Y'_1+Y'_2 & 0 & -N\\
N & 0 & \vec{Z}''_a+Z''_1+Z''_2 & Z''_2\\
0 & -N & Z''_2 & Z''_a+Z''_1+Z''_2
\end{vmatrix}=0 \quad (38)$$

where

$$\vec{Y}_a' = Y_a' \frac{jY_a' + Y_L' \cot(k_{ya}d)}{Y_a' \cot(k_{ya}d) + jY_L'} \quad (39)$$

and

$$\vec{Z}_a'' = Z_a'' \frac{jZ_a'' + Z_L'' \cot(k_{ya}d)}{Z_a'' \cot(k_{ya}d) + jZ_L''}. \quad (40)$$

Y_a' and Z_a'' are given by the reciprocals of (A4) and (A10) of the Appendix, and Y_L', Z_L'', and N^2 are given by (36), (35), and (16), respectively. The pi and tee equivalent parameters of the transmission lines within the dielectric region are given in [14] and written here for convenience as

$$Y_1' = jY_\epsilon' \tan(k_{y\epsilon}b/2) \qquad Y_2' = -jY_\epsilon' \csc(k_{y\epsilon}b) \quad (41)$$

where Y_ϵ' is given by the reciprocal of (A4) with ϵ_r being the dielectric constant of the strip, and

$$Z_1'' = jZ_\epsilon'' \tan(k_{y\epsilon}b/2) \qquad Z_2'' = -jZ_\epsilon'' \csc(k_{y\epsilon}b) \quad (42)$$

where Z_ϵ'' is given by the reciprocal of (A10).

The compatibility condition (38) reduces itself to a much simpler form when the antenna can radiate from both sides and the strip is located at the middle point of the parallel plates so that the structure is symmetrical. We replace Y_a' and Z_a'' by $\vec{Y}_a'$ and $\vec{Z}_a''$ in the determinantal equation (38), and after simple algebraic manipulations, (38) factorizes to either

$$\left(\vec{Z}_a'' + Z_1''\right)\left(\vec{Y}_a' + Y_1' + 2Y_2'\right) = N^2 \quad (43)$$

or

$$\left(\vec{Y}_a' + Y_1'\right)\left(\vec{Z}_a'' + Z_1'' + 2Z_2''\right) = N^2 \quad (44)$$

which can be written in a more revealing form, after using (41) and (42) and simple trigonometric identities, as either

$$\left(\vec{Z}_a'' + jZ_\epsilon'' \tan(k_{y\epsilon}b/2)\right)\left(\vec{Y}_a' - jY_\epsilon' \cot(k_{y\epsilon}b/2)\right) = N^2 \quad (45)$$

or

$$\left(\vec{Y}_a' + jY_\epsilon' \tan(k_{y\epsilon}b/2)\right)\left(\vec{Z}_a'' - jZ_\epsilon'' \cot(k_{y\epsilon}b/2)\right) = N^2. \quad (46)$$

One can readily recognize that (45) and (46) correspond to leaky modes with a short circuit or an open circuit at the plane of symmetry. The antenna is operated in the lowest mode, which is the one corresponding to the short-circuit condition.

IV. Numerical Results

Using the dispersion relation (38), we have obtained the values of the phase constant β and the leakage constant α as a function of various geometric parameters. These quantities are the ones we need in order to design the antenna in response to performance requirements. The dispersion relation was solved by a numerical procedure that requires a first estimate of the root searched for. In most cases, the estimate was taken from the value of β for the nonradiating case for which the dispersion relation is simple and yields real roots. A typical number of five iterations was enough to achieve convergence, and double precision was required to obtain accurately the values of α.

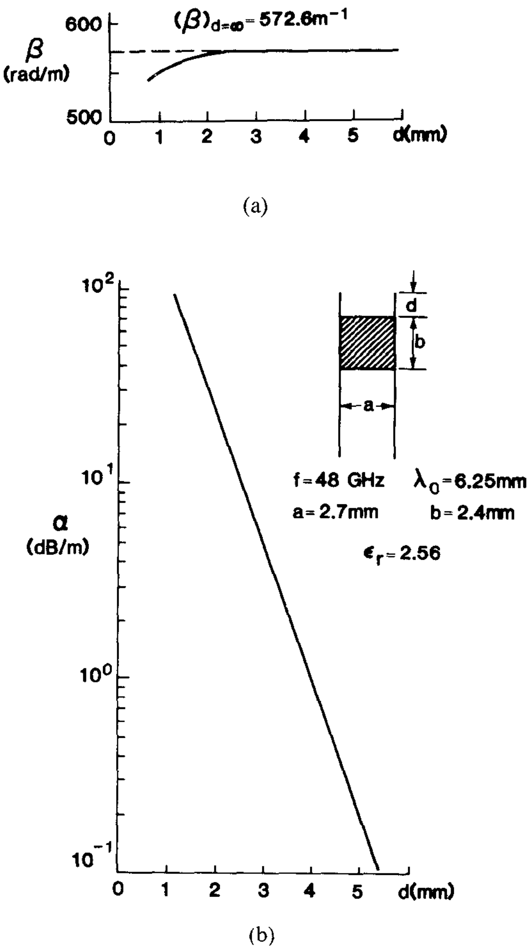

Fig. 8. (a) Phase constant β in radians/meter of the leaky-wave structure in Fig. 2 as a function of d in mm, showing that β is independent of d beyond some minimum value of d. (b) Leakage constant α in dB/meter of the leaky-wave structure in Fig. 2 as a function of the distance d in mm between the dielectric strip and the radiating open end.

For simplicity in design, one desires that β remain constant while α varies as a function of a specific parameter. In that way, the geometry can be changed to alter α without changing β, thereby permitting one to taper the amplitude distribution and simultaneously maintain the phase linear along the antenna aperture length. The variations of α and β with d, the distance between the air–dielectric interface and the radiating open end, satisfy this requirement provided d remains greater than some minimum value. Figs. 8(a) and 8(b) present these dependences, and show that for $d > 2$ mm, β remains essentially unchanged, as desired. It is also seen that α increases as d is shortened, as expected since the field decays exponentially away from the dielectric region. Thus, the value of α that one can achieve spans a very large range. The results in Figs. 8(a) and 8(b) correspond to a set of geometric and constitutive parameters given by Yoneyama and Nishida in their original paper [1] on NRD guide.

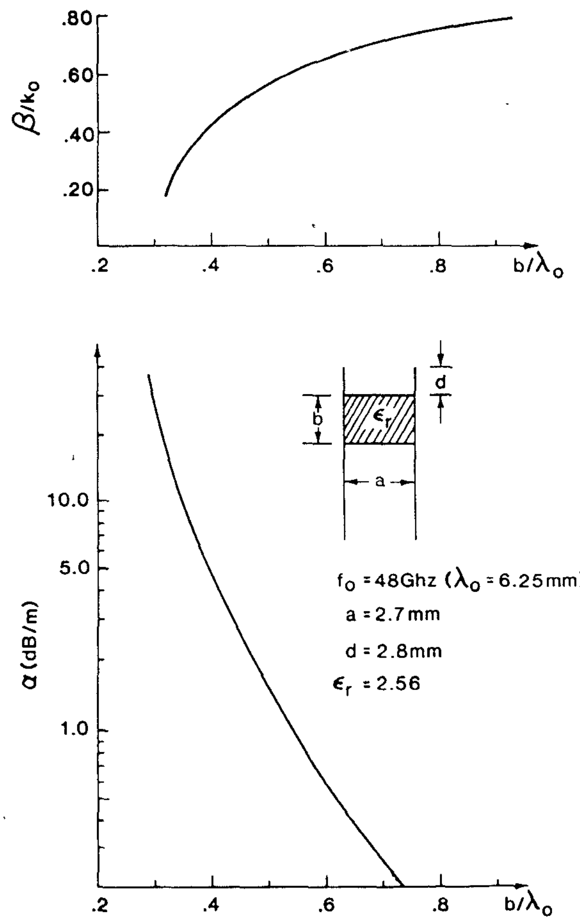

Fig. 9. Curves of phase constant β and leakage constant α as a function of the thickness b of the dielectric strip, for the foreshortened-top NRD guide antenna.

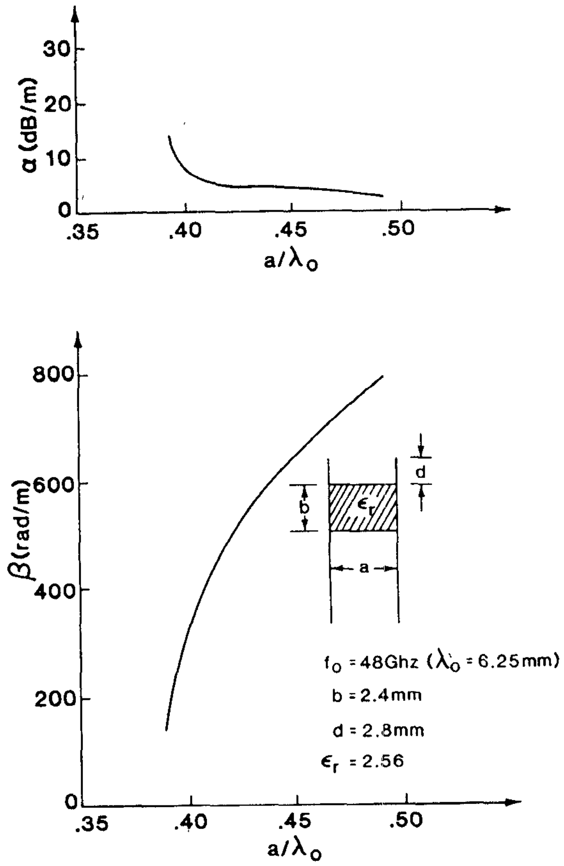

Fig. 10. Curves of leakage constant α and phase constant β as a function of the plate spacing a, for the foreshortened-top NRD guide antenna.

The dependence of α and β on the *thickness of the dielectric strip* appears in Fig. 9. These calculated curves were found, as mentioned above, from the dispersion relation (38) of the complete network. Here, both α and β change as b is varied. Most significantly, the leakage constant α decreases as the strip becomes thicker. This behavior is to be expected physically, since a thicker dielectric strip produces a greater field confinement to the region of the strip; as a result, the field amplitude at the radiating open end is less and, in turn, less leakage power is produced.

The variations of α and β with the *separation between the plates* are given in Fig. 10. For convenience, the curves were calculated with the dispersion relation in (45), which corresponds to a symmetrical structure with a short-circuit bisection, but taking the radiation from one end only. Comparisons for specific points computed from the complete and asymmetric structure show that the differences are very small in the range of α values used in these curves. Here, we find an inverse situation, but as expected. As one varies the plate separation, the value of β changes greatly, but α changes only little, except near cutoff. In fact, α remains flat over a reasonably wide range of a/λ_0. The dependences permit the designer to vary spacing a to adjust β and, therefore, the angle of the radiated beam, and to vary d to adjust α and, therefore, the beamwidth. The variation of α versus a in Fig. 10 also implies that a small variation in plate spacing will negligibly affect the sidelobe distribution.

The last parameter that can be varied is the *dielectric constant* ϵ_r of the dielectric strip; the effects of ϵ_r on α and β are shown in Fig. 11. The curves were calculated in the same fashion as those in Fig. 10, using the dispersion relation corresponding to the bisected structure having a short circuit at the bisecting plane. It is interesting that the leakage constant varies two orders of magnitude between cutoff and the onset of the slow-wave region, and that this whole range can be spanned by changing ϵ_r from 2.0 to 3.4. Furthermore, a strip with $\epsilon_r = 2.20$ can have roughly double the leakage of a strip of the same dimensions but composed of polystyrene with $\epsilon_r = 2.56$. This decay of α with increasing ϵ_r is readily understood physically since the fields are more confined for higher ϵ_r values, so that less field arrives at the antenna aperture, and the leakage is reduced. We note that the normalized phase constant β/k_0 changes greatly with ϵ_r, as expected, but also that the variation is linear over a wide range of values of ϵ_r when the guide is away from cutoff.

V. Conclusions

We have shown that a leaky waveguide can be readily fabricated with nonradiative dielectric (NRD) waveguide, and we have presented a very accurate theory that provides

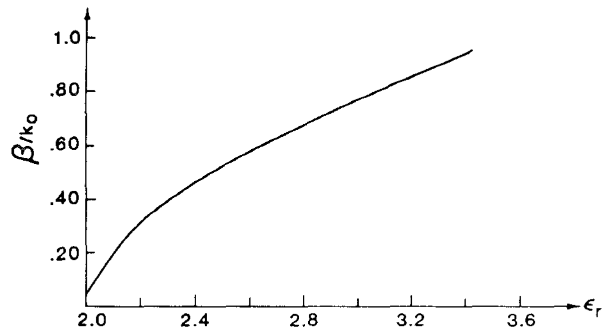

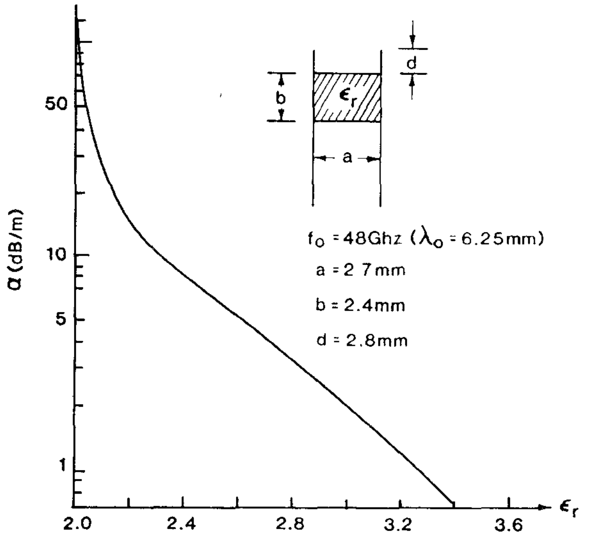

Fig. 11. Curves of phase constant β and leakage constant α as a function of the relative dielectric constant ϵ_r of the dielectric strip, for the foreshortened-top NRD guide antenna.

its leakage and phase constants in closed form. Curves displaying the variations of the leakage and phase constants as a function of all the geometric and constitutive parameters were calculated using this accurate theory, and are also given here. Careful measurements were also taken of the leakage constant for several different frequencies and geometric parameters. A description of the experimental setup and comparisons between these measurements and our accurate theory are presented in the companion paper, part II.

Appendix
E-Type and H-Type Mode Functions for Parallel-Plate Guide

The mode functions presented here are those appropriate to the perfectly conducting parallel-plate guide sections making up the NRD guide in Fig. 1 and the leaky-wave structure in Fig. 2(a), when the field variation along z is such that $\partial/\partial z \to -j\beta$. Since in this case the variation in z is consistently $\exp(-j\beta z)$, the z dependence is suppressed. From the wave equation for e_z' and h_z'' and the vector eigenvalue problem for the vectorial functions $\boldsymbol{e}'$ and $\boldsymbol{h}''$ [7], one obtains the relations below.

$E^{(z)}$-type modes:

$$H_{xn}' = I_n'(y)h_{xn}' = I_n'(y)\sqrt{2/a}\,\sin\left(\frac{n\pi x}{a}\right) \quad \text{(A1)}$$

$$E_{zn}' = V_n'(y)e_{zn}' = V_n'(y)\sqrt{2/a}\,\sin\left(\frac{n\pi x}{a}\right) \quad \text{(A2)}$$

$$E_{xn}' = V_n'(y)e_{xn}' = V_n'(y)\left(\frac{-j\beta}{\epsilon_r k_0^2-\beta^2}\right)\frac{n\pi}{a}\sqrt{2/a}\,\cos\left(\frac{n\pi x}{a}\right) \quad \text{(A3)}$$

$$Z_n' = \frac{\epsilon_r k_0^2-\beta^2}{k_{yn}'\omega\epsilon_0\epsilon_r} \qquad (\epsilon_r = 1 \text{ for air regions}) \quad \text{(A4)}$$

$$H_{yn}' = -\frac{1}{j\omega\mu_0}(\nabla\times\boldsymbol{E}_n')_y = \frac{\omega\epsilon_0\epsilon_r}{\beta}E_{xn}' \quad \text{(A5)}$$

$$E_{yn}' = \frac{1}{j\omega\epsilon_0\epsilon_r}(\nabla\times\boldsymbol{H}_n')_y = -\frac{\beta}{\omega\epsilon_0\epsilon_r}H_{xn}'. \quad \text{(A6)}$$

$H^{(z)}$-type modes:

$$H_{zn}'' = I_n''(y)h_{zn}'' = I_n''(y)\sqrt{2/a}\,\cos\left(\frac{n\pi x}{a}\right) \quad \text{(A7)}$$

$$E_{xn}'' = V_n''(y)e_{xn}'' = V_n''(y)\left(-\sqrt{2/a}\,\cos\left(\frac{n\pi x}{a}\right)\right) \quad \text{(A8)}$$

$$H_{xn}'' = I_n''(y)h_{xn}'' = I_n''(y)\left(\frac{j}{\epsilon_r k_0^2-\beta^2}\right)\frac{n\pi}{a}\sqrt{2/a}\,\sin\left(\frac{n\pi x}{a}\right) \quad \text{(A9)}$$

$$Y_n'' = \frac{\epsilon_r k_0^2-\beta^2}{k_{yn}''\omega\mu_0} \qquad (\epsilon_r = 1 \text{ for air regions}) \quad \text{(A10)}$$

$$E_{yn}'' = \frac{1}{j\omega\epsilon_0\epsilon_r}(\nabla\times\boldsymbol{H}_n'')_y = -\frac{\omega\mu_0}{\beta}H_{xn}'' \quad \text{(A11)}$$

$$H_{yn}'' = \frac{-1}{j\omega\mu_0}(\nabla\times\boldsymbol{E}_n'')_y = \frac{\beta}{\omega\mu_0}E_{xn}''. \quad \text{(A12)}$$

Acknowledgment

The authors gratefully acknowledge the helpful discussions maintained with Dr. H. Shigesawa, Dr. S. Ohkawa, and Dr. Z. Y. Shen.

References

[1] T. Yoneyama and S. Nishida, "Nonradiative dielectric waveguide for millimeter-wave integrated circuits," *IEEE Trans. Microwave Theory Tech.*, vol MTT-29, pp. 1188–1192, Nov. 1981.
[2] T. Yoneyama and S. Nishida, "Nonradiative dielectric waveguide circuit components," presented at the Int. Conf. Infrared and Millimeter Waves, Miami, FL, Dec. 1981.
[3] T. Yoneyama, F. Kuroki, and S. Nishida, "Design of nonradiative dielectric waveguide filters," *IEEE Trans. Microwave Theory Tech.*, vol. MTT-32, pp. 1659–1662, Dec. 1984.
[4] P. J. B. Clarricoats and A. A. Oliner, "Transverse-network representation for inhomogeneously filled circular waveguides," *Proc. Inst. Elec. Eng.*, vol. 112, no. 5, pp. 883–894, 1965.
[5] H. Shigesawa and K. Takiyama, "Study of a leaky H-guide," presented at the Int. Conf. Microwaves, Circuit Theory and Information, Tokyo, Japan, 1964.

[6] K. Takiyama and H. Shigesawa, "The radiation characteristics of a leaky *H*-guide," *J. Inst. Electron. Commun. Eng. Jap.*, vol. 50, no. 2, pp. 181–188, 1967.
[7] K. Takiyama and H. Shigesawa, "On the study of a leaky *H*-guide," *Sci. and Eng. Rev. Doshisha Univ.*, vol. 7, no. 4, pp. 203–225, 1967.
[8] H. Shigesawa, K. Fujiyama, and K. Takiyama, "Complex propagation constants in leaky waveguides with rectangular cross section," presented at scientific conference, Japan, July 3, 1970.
[9] L. A. Weinstein, *The Theory of Diffraction and the Factorization Method* (translated from Russian). Boulder, CO: Golem Press, 1969, pp. 29–50.
[10] N. Marcuvitz, "Radial transmission lines," ch. 8 of *Principles of Microwave Circuits* (vol. 8 of MIT Radiation Laboratory Series). New York: McGraw Hill, 1948.
[11] A. Sanchez, "A leaky-wave antenna for millimeter waves using non-radiative dielectric waveguide," Ph.D. thesis, Polytechnic Institute of New York, June 1983.
[12] H. M. Altschuler and L. O. Goldstone, "On network representations of certain obstacles in waveguide regions," IRE *Trans. Microwave Theory Tech.*, vol. MTT-7, pp. 213–221, Apr. 1959.
[13] N. Marcuvitz, *Waveguide Handbook*, (vol. 10 of MIT Radiation Laboratory Series). New York: McGraw-Hill, 1951, p. 4.
[14] N. Marcuvitz, *Waveguide Handbook* (vol. 10 of MIT Radiation Laboratory Series). New York: McGraw-Hill, 1951, p. 12.

Alberto Sanchez (S'81–M'82) was born in Zaragoza, Spain, in 1944. He received the degree of Licenciado en Fisica from the University of Zaragoza, Spain, in 1970 and the M.S. in electrophysics and the Ph.D. in electrical engineering from the Polytechnic Institute of New York in 1978 and 1983, respectively. From 1977 to 1982, he was engaged in research on millimeter-wave and optical integrated circuits as a research assistant with the Microwave Research Institute of the Polytechnic Institute of New York.

He joined the RCA Laboratories, Princeton, NJ, in 1982, where he was involved in the development of active printed circuit antenna arrays for Direct Broadcast Satellites (DBS) until 1986. He transferred to RCA Astro-Space Division in 1986, where he has been involved in different projects in beam forming network waveguide component design, dielectrically loaded horns, printed circuit antenna array feeds for MobilSat, and computer simulation of spacecraft electromagnetic interference.

Dr. Sanchez received the "Fundación Juan March" Scholarship for Advanced Studies in the U.S. in 1975. He is a member of the IEEE Microwave Theory and Techniques Society and the IEEE Antennas and Propagation Society.

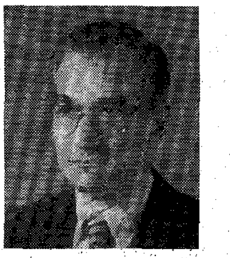

Arthur A. Oliner (M'47–SM'52–F'61–LF'87) was born in Shanghai, China, on March 5, 1921. He received the B.A. degree from Brooklyn College, Brooklyn, NY, and the Ph.D. degree from Cornell University, Ithaca, NY, both in physics, in 1941 and 1946, respectively.

While at Cornell University, he held a Graduate Teaching Assistantship in the Physics Department and also conducted research on a project of the Office of Scientific Research and Development. He joined the Microwave Research Institute of the Polytechnic Institute of Brooklyn, Brooklyn, NY, in 1946, and was made Professor in 1957. From 1966 to 1971, he was Head of the Electrophysics Department; he then became Head of the combined Department of Electrical Engineering and Electrophysics from 1971 through 1974. He was also the Director of the Microwave Research Institute from 1967 to 1981. During the summer of 1964, he was a Walker–Ames Visiting Professor at the University of Washington, Seattle, and during the 1965–1966 academic year, he was on sabbatical leave at the Ecole Normale Supérieure, Paris, France, under a Guggenheim Fellowship. During the summer of 1973, he was a Visiting Professor at the Catholic University, Rio de Janeiro, Brazil; in the spring of 1978 he was a Visiting Research Scholar at the Tokyo Institute of Technology, Japan; in the spring of 1980 he was a Visiting Professor at the Huazhong (Central China) Institute of Technology, Wuhan, China; and in the fall of 1982 he was a Visiting Professor at the University of Rome "La Sapienza," Rome, Italy. He has been engaged in research in a wide variety of topics in the microwave field, including network representations of microwave structures, precision measurement methods, guided-wave theory with stress on surface waves and leaky waves, traveling-wave antennas, plasmas, periodic structure theory, and phased arrays. His interests have also included waveguides for surface acoustic waves and integrated optics and, more recently, guiding and radiating structures for the millimeter and near-millimeter wave ranges. He is the author of over 150 papers, and coauthor or coeditor of three books. He served on the Editorial Boards of the journal *Electronics Letters* (published by the British IEE) and the volume series *Advances in Microwaves* (Academic Press).

Dr. Oliner is a Fellow of the AAAS and the British IEE, and he served as the first MIT National Lecturer in 1967. He has received prizes for two of his papers: the IEEE Microwave Prize in 1967 and the Institution Premium, the highest award of the British IEE, in 1964. He was named an Outstanding Educator of America in 1973, and in 1974 he received a Sigma Xi Citation for Distinguished Research. He was a National Chairman of the IEEE MTT Society, a member of the IEEE Publication Board, and General Chairman of three symposia. In 1977 he was elected an Honorary Life Member of the IEEE MTT Society, and in 1982 he received the IEEE Microwave Career Award. In 1984, he was a recipient of the IEEE Centennial Medal. He is a member of several Commissions of the International Union of Radio Science (URSI), a past Chairman of Commission 1 (now A), and presently USA Chairman of Commission D. He is also a former Chairman of a National Academy of Sciences Advisory Panel to the National Bureau of Standards.